Published in final edited form as:
J Am Chem Soc. 2009 December 2; 131(47): 17093–17095. doi:10.1021/ja902293w.

Buckyballs meet Viral Nanoparticles – Candidates for Biomedicine

Nicole F. Steinmetz[†,*], **Vu Hong**[‡], **Erik D. Spoerke**[⊥], **Ping Lu**[¥], **Kurt Breitenkamp**[‡], **M.G. Finn**[‡,*], and **Marianne Manchester**[†,*]

[†]Department of Cell Biology and Center for Integrative Molecular Biosciences, The Scripps Research Institute, 10550 North Torrey Pines Road, La Jolla, California 92037, USA

[‡]Department of Chemistry and The Skaggs Institute for Chemical Biology, The Scripps Research Institute, 10550 North Torrey Pines Road, La Jolla, California 92037, USA

[⊥]Department of Electronic and Nanostructured Materials, Sandia National Laboratory, Albuquerque, New Mexico 87185, USA

[¥]Department of Materials Characterization, Sandia National Laboratory, Albuquerque, New Mexico 87185, USA

Abstract

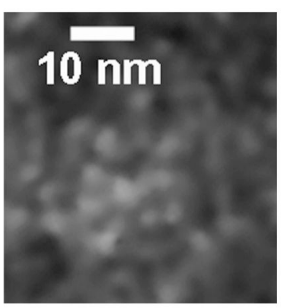

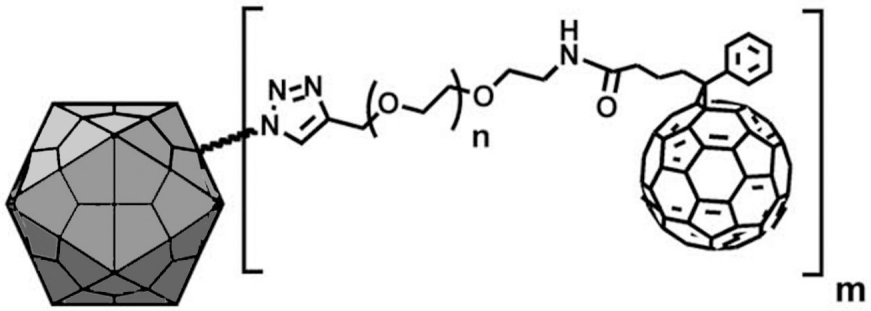

Fullerenes such as C_{60} show promise as functional components in several emerging technologies. For biomedical applications, C_{60} has been used in gene- and drug-delivery vectors, as imaging agents, and as photosensitizers in cancer therapy. A major drawback of C_{60} for bioapplications is its insolubility in water. To overcome this limitation, we covalently attached C_{60} derivatives to *Cowpea mosaic virus* and bacteriophage Qβ virus-like particles, as examples of naturally occurring viral nanoparticle (VNP) structures that have been shown to be promising candidates for biomedicine. Two different labeling strategies were employed, giving rise to water-soluble and stable VNP-C_{60} and VNP-PEG-C_{60} conjugates. Samples were characterized using a combination of transmission electron microscopy, scanning transmission electron microscopy (STEM), gel electrophoresis, size-exclusion chromatography, dynamic light scattering, and western blotting. “Click” chemistry bioconjugation using a PEG-modified propargyl-O-PEG-C_{60} derivative gave rise to high loadings of fullerene on the VNP surface, indicated by the imaging of individual C_{60} units by STEM. The cellular uptake of dye-labeled VNP-PEG-C_{60} complexes in a human cancer cell line was found by confocal microscopy to be robust, showing that cell internalization was not inhibited by the attached

nicoles@scripps.edu, mgfinn@scripps.edu, and marim@scripps.edu.

Supporting Information Available: Experimental details and supporting Figures. This material is available free of charge via the Internet at http://pubs.acs.org.

C_{60} units. These results open the door for the development of novel therapeutic devices with potential applications in photo-activated tumor therapy.

The fullerene class of carbon allotropes shows promise as functional components in several emerging technologies. Properties such as high electron affinity and charge transport capabilities have made derivatives of C_{60} (aka Buckyball) and carbon nanotubes particularly attractive for next generation photovoltaic and electrical energy storage devices.[1] More recently, there has been increased interest in studying fullerenes for use in biomedicine. C_{60} has been used in gene-delivery vectors, HIV-1 protease inhibitors, magnetic resonance imaging agents, and drug-delivery.[2] Due to its exceptional radical-scavenging properties, C_{60} is a promising candidate for photosensitizers in cancer therapy and the treatment of inflammatory diseases.[3]

A major drawback of C_{60} for biological applications is its insolubility in water, and numerous modifications have been made to increase its aqueous biocompatibility.[4] We describe the alternative approach of covalently attaching C_{60} derivatives to a larger biological structure, in this case viral nanoparticles (VNPs). VNPs are naturally occurring self-assembling protein structures with potential applications ranging from materials to biomedicine.[5] Here we employ *Cowpea mosaic virus* (CPMV) and the capsid of bacteriophage Qβ (Fig. 1A), both of which are 30 nm in size and have icosahedral symmetry. Qβ is formed from 180 copies of a single coat protein subunit, while CPMV is composed of 60 copies of two different coat proteins, designated the large (L) and small (S) subunits. The capsid of each VNP offers multivalent attachment sites at solvent-exposed amino acids, on which diverse molecules such as redox-active moieties, imaging agents, and targeting ligands have been previously displayed.[5] The generation of aggregates of single-walled carbon nanotubes and *Flock House virus* has been reported.[6]

We envisioned that VNPs could serve both as hydrophilic "chaperones" for C_{60}, making the fullerene water soluble, and as platforms for the organized assembly of multiple C_{60} units in combination with other functional molecules. The specific, localized binding of C_{60} to VNP scaffolds could resolve problems of aggregation and cluster formation common to unbound fullerene derivatives. The goal of this study was to determine whether the advantages of fullerenes and VNPs could be combined by covalently attaching C_{60} derivatives to CPMV and Qβ. To test the potential of the hybrid nanomaterials as candidates for biomedical applications such as photodynamic tumor therapy, the cellular uptake of VNP-C_{60} complexes in a human cancer cell lines was studied.

The VNPs were decorated with C_{60} in two ways. First, the well-characterized fullerene derivative 1-(3-carboxypropyl)-1-phenyl-[6,6]C_{61} (PCBA) was activated by carbodiimide-N-hydroxysuccinimide chemistry and coupled to solvent-exposed Lys residues on CPMV and Qβ (Fig. 1B and Supp. Info.). Second, we employed the copper-catalyzed azide-alkyne cycloaddition (CuCAAC) "click" reaction,[7] which has found wide application due to its high rate and specificity. CuAAC protocols have been developed and improved in the past several years for the attachment of functional molecules to VNPs with high loadings.[8] In the present case, a propargyl-O-PEG-C_{60} derivative was synthesized and conjugated to azide-modified Qβ particles using an optimized procedure[8a] (Fig. 1C and Supp. Info), resulting in significantly higher loading than the attachment of PCBA using activated ester chemistry. In both cases, the existence of only a single linker group on each C_{60} derivative prevented covalent aggregation of the nanoparticles. The resulting hybrid complexes (VNP-C_{60} and VNP-PEG-C_{60}) were soluble and stable in aqueous buffer solutions for at least several months.

VNP-C_{60} and VNP-PEG-C_{60} samples were characterized by a combination of techniques. Size-exclusion chromatography (SEC, Fig. 1D,E), transmission electron microscopy (TEM,

Figure 1M,N), scanning transmission electron microscopy (STEM, Fig. 1O), and native gel electrophoresis (Supp. Info.) of VNP-C_{60} particles confirmed their intact nature with no detectable decomposition. The covalent attachment of C_{60} was verified in both cases by western blotting using an anti-C_{60} antibody (Fig. 1H,I) and in case of Qβ also by STEM (Fig. 1O). Dynamic light scattering (DLS, Fig. 1J) showed no significant changes in the apparent size of CPMV and Qβ upon attachment of C_{60}, consistent with low coverage (see below). SEC of Qβ and Qβ-C_{60} showed no change in retention time, whereas CPMV exhibited a change in retention time upon fullerene attachment (23.9 min to 26.0 min). These differing SEC comparisons may reflect differing chemical interactions with the chromatography stationary phase that complicate the correlation between retention time and size. C_{60} is perhaps unusual in this respect, since it is spherical and hydrophobic. Interestingly, C_{60} moieties were found attached only to the S protein of CPMV (Fig. 1I), presumably at the highly reactive K38 residue.[9]

Similarly, the click reaction to prepare Qβ-PEG-C_{60} gave a mixture of intact particles (peak b in Fig. 1F) plus aggregated material (peak a) and broken particles (peak c). No interaction was observed between Qβ-azide and propargyl-O-PEG-C_{60} in the absence of Cu^{I}, supporting the covalent nature of the derivatization. Intact Qβ-PEG-C_{60} particles were purified by SEC and reanalyzed (Fig. 1G), showing a shift to shorter retention time compared to the underivatized particle (28.9 min to 28.1 min), consistent with an increase in size upon C_{60} attachment. TEM (Fig. 1P), STEM (Fig. 1Q), and native gels (Supp. Info.) further confirmed the structural integrity of the Qβ-PEG-C_{60} conjugate. The hydrodynamic radius of the particle was found by DLS to increase from 13.1 nm for unmodified Qβ to 16.7 nm for Qβ-PEG-C_{60}, in good agreement with the expected dimensions of the attached species (1 nm diameter for C_{60} plus approximately 2.3 nm length of the PEG-1000 chain, see Supporting Information).

Covalent attachment of PEG-C_{60} to Qβ was further verified by the appearance of two distinct bands on denaturing gel electrophoresis, corresponding to non-labeled and PEG-C_{60}-conjugated coat proteins (Fig. 1K). Western blotting was attempted but was not successful, which may be due to blocking of the antibody-fullerene interaction by the PEG chains (not shown).

A combination of techniques was used to quantify the degree of C_{60} loading. STEM (Fig. 1O) and UV-vis absorbance (332 nm, Supp. Info.) indicated sparse decoration of Qβ (approximately 3 C_{60} molecules per particle) with PCBA using carbodiimide chemistry. This modest loading level derives from the relative aqueous insolubility of PCBA and the modest rates of amine-NHS ester reactions, and is presumably similar for the analogous CPMV reactions.

In contrast, Qβ-PEG-C_{60} showed a much higher level of coverage. Individual C_{60} particles were easily visualized in large numbers around each VLP as dots of bright contrast in STEM images after osmium tetroxide staining (Fig. 1Q). UV-vis absorbance spectroscopy (332 nm, Supp. Info.) indicated a loading of 45–50 C_{60} molecules per Qβ particle. Quantitative comparison of the intensities of the derivatized and unlabeled protein bands in denaturing protein gels after Coomassie staining (Fig. 1K) gave rise to a similar estimate of 30–40 C_{60} molecules per Qβ-PEG-C_{60} conjugate. The significantly greater loading is likely the result of better solubility of the PEGylated C_{60} reagent in the aqueous reaction mixture and the higher efficiency of the CuAAC reaction.

To evaluate the potential of the hybrid nanomaterials as candidates for biomedical applications, cellular uptake of dye-labeled VNP-C_{60} (not shown) and VNP-PEG-C_{60} complexes in the HeLa human cancer cell line was studied using confocal microscopy (Fig. 2 and Supp. Info.) Qβ-PEG-C_{60} was labeled with approximately 60 AlexaFluor568 (A568) fluorophores per particle in a second CuAAC reaction (Supp. Info.), with dye attachment being confirmed by

UV-vis, SEC, and native and denaturing gel electrophoresis (Supp. Info.). Cellular uptake was revealed by the acquisition of Z-dimensional fluorescence data (Fig. 2), and was found to be the same as for analogous Qβ particles bearing only the dye (data not shown), showing that internalization was not inhibited by the attached C_{60} units.

In conclusion, we have demonstrated that modified fullerene and protein nanoparticles can be covalently linked to each other with high efficiency by click chemistry, retaining the structural, spectroscopic, and biological properties of each. The hybrid VNP-C_{60}/VNP-PEG-C_{60} complexes were water-soluble and biocompatible, and the VNPs serve as scaffolds and vehicles for detectable C_{60}-delivery into cells. This opens the door for the development of novel therapeutic devices with potential applications in photo-activated tumor therapy. Studies along these lines are currently under investigation in our laboratories.

Supplementary Material

Refer to Web version on PubMed Central for supplementary material.

Acknowledgments

We thank Dr. So-Hye Cho and Dr. Rebecca Taurog for TEM studies. This work was supported by the NIH 1K99EB009105 (to N.F.S), R01CA112075 (to MM and MGF), RR021886 (to MGF), the American Heart Association (postdoctoral fellowship to NFS), and the W.M. Keck Foundation. Work at Sandia National Labs was funded by Sandia's Laboratory Directed Research and Development Program and the Department of Energy Basic Energy Sciences Program. Sandia is a multiprogram laboratory operated by Sandia Corporation, a Lockheed Martin Company, for the United States Department of Energy's National Nuclear Security Administration under Contract DE-AC04-94AL85000.

REFERENCES

1. (a) Thompson BC, Frechet JM. Angew Chem Int Ed Engl 2008;47:58–77. [PubMed: 18041798] (b) Taylor R, Walton D. Nature 1993;363:685–693.
2. (a) Bosi S, Da Ros T, Spalluto G, Prato M. Eur J Med Chem 2003;38:913–923. [PubMed: 14642323] (b) Nielsen GD, Roursgaard M, Jensen KA, Poulsen SS, Larsen ST. Basic Clin Pharmacol Toxicol 2008;103:197–208. [PubMed: 18684229]
3. (a) Mroz P, Pawlak A, Satti M, Lee H, Wharton T, Gali H, Sarna T, Hamblin MR. Free Radic Biol Med 2007;43:711–719. [PubMed: 17664135] (b) Qu X, Komatsu T, Sato T, Glatter O, Horinouchi H, Kobayashi K, Tsuchida E. Bioconjugate Chem 2008;19:1556–1560. (c) Zhao B, He YY, Bilski PJ, Chignell CF. Chem Res Toxicol 2008;21:1056–1063. [PubMed: 18422350]
4. (a) Andersson T, Westman G, Wennerstroem O, Sundhahl M. J. Chem. Soc. Perkin Trans 1994;2:1097–1101. (b) Hummelen J, Knight B, LePeq F, Wudl F. J. Org. Chem 1995;60:532–538. (c) Sijbesma R, Srdanov G, Wudl F, Castoro J, Wilkins C, Friedman S, DeCamp D, Kenyon G. J.Am Chem. Soc 1993;115:6510–6512. (d) Sitharaman B, Zakharian T, Saraf A, Misra P, Ashcroft J, Pan S, Pham Q, Mikos A, Wilson L, Engler D. Mol. Pharm 2008;5:567–578. [PubMed: 18505267] (e) Vasella A, Uhlmann P, Waldruff C, Diederich F, Thilgen C. Angew. Chem, Int, Ed 1992;31:1388–1390.
5. (a) Manchester, M.; Steinmetz, NF. Viruses and Nanotechnology. Vol. Vol. 327. Berlin Heidelberg: Springer Verlag; 2008. (b) Young M, Willits D, Uchida M, Douglas T. Annu Rev Phytopathol 2008;46:361–384. [PubMed: 18473700]
6. Portney NG, Singh K, Chaudhary S, Destito G, Schneemann A, Manchester M, Ozkan M. Langmuir 2005;21:2098–2103. [PubMed: 15751992]
7. (a) Kolb HC, Finn MG, Sharpless KB. Angew Chem Int Ed 2001;40:2004–2021. (b) Tornøe CW, Christensen C, Meldal M. J. Org. Chem 2002;67:3057–3062. [PubMed: 11975567] (c) Rostovtsev VV, Green LG, Fokin VV, Sharpless KB. Angew. Chem. Int. Ed 2002;41:2596–2599.
8. (a) Hong V, Presolski SI, Ma C, Finn MG. Angew. Chem. Int. Ed. 2009 in press. (b) Bruckman MA, Kaur G, Lee LA, Xie F, Sepulveda J, Breitenkamp R, Zhang X, Joralemon M, Russell TP, Emrick T, Wang Q. ChemBioChem 2008;9:519–523. [PubMed: 18213566] (c) Sen Gupta S, Kuzelka J, Singh P, Lewis WG, Manchester M, Finn MG. Bioconjugate Chem 2005;16:1572–1579. (d) Wang Q, Chan

TR, Hilgraf R, Fokin VV, Sharpless KB, Finn MG. J Am Chem Soc 2003;125:3192–3193. [PubMed: 12630856]

9. (a) Chatterji A, Ochoa W, Paine M, Ratna BR, Johnson JE, Lin T. Chem Biol 2004;11:855–863. [PubMed: 15217618] (b) Wang Q, Kaltgrad E, Lin T, Johnson JE, Finn MG. Chem Biol 2002;9:805–811. [PubMed: 12144924] (c) Steinmetz NF, Evans DJ, Lomonossoff GP. ChemBioChem 2007;8:1131–1136. [PubMed: 17526061]

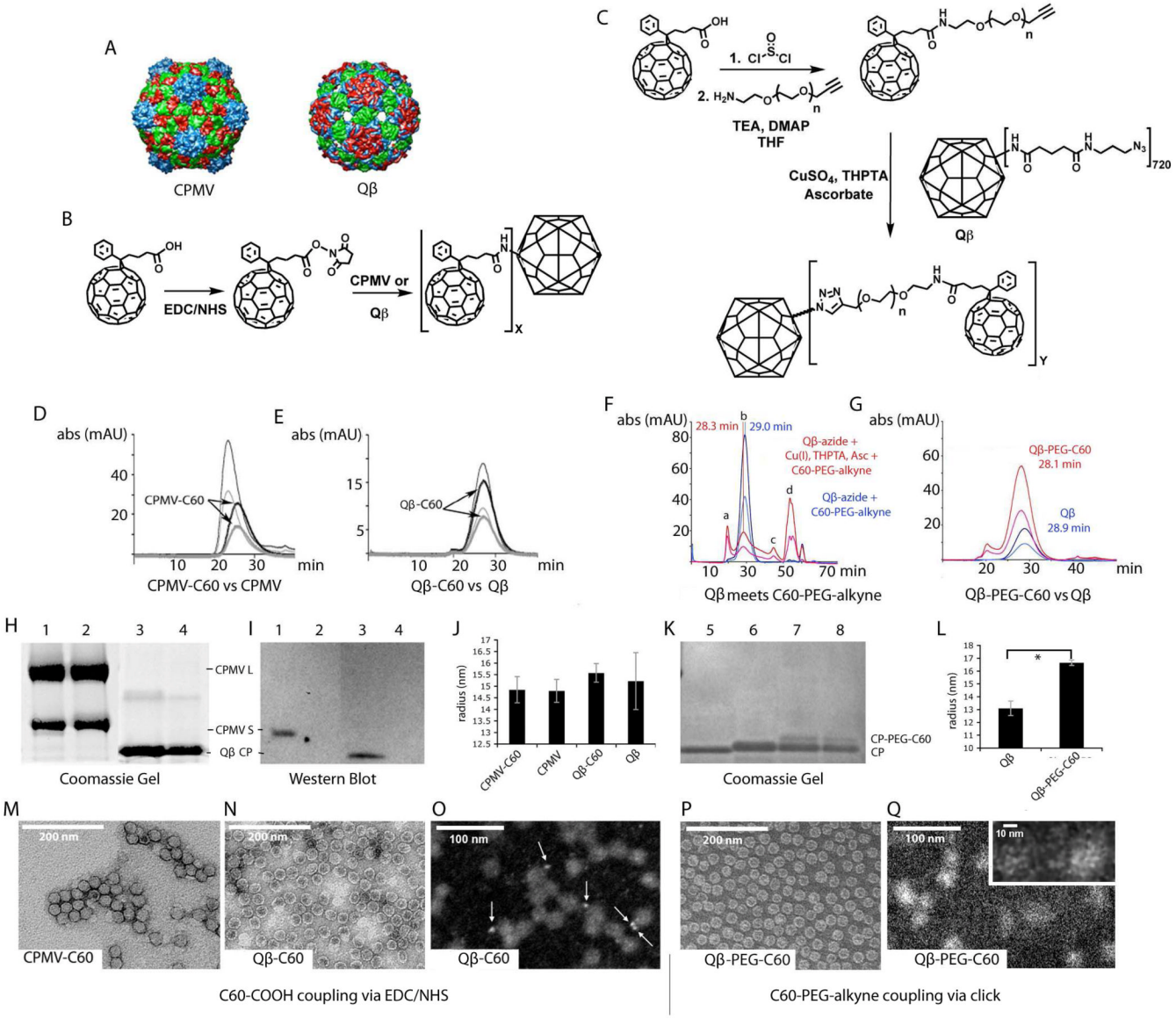

Figure 1.

(A) Structure of CPMV and Qβ (reproduced from VIPERdb). (B) Derivatization of CPMV and Qβ with PCBA. (C) Derivatization of Qβ with propargyl-O-PEG-C_{60}; THPTA = tris(3-hydroxypropyl-4-triazolylmethyl)amine as an accelerating Cu-binding ligand, n = average of 20. (D, E) SEC using a Superose 6 column (black line = absorbance at 260 nm, grey line = absorbance at 280 nm). (F) SEC of Qβ mixed with propargyl-O-PEG-C_{60} (dark blue line = 260 nm, light blue line = 280 nm) vs. Qβ reacted with propargyl-O-PEG-C_{60} in presence of $CuSO_4$, THPTA, and Na ascorbate (red line = 260 nm, pink line = 280 nm). Peak a (19.6 min) = VNP aggregates, b (28.3 and 29.0 min) = intact Qβ-PEG-C_{60} and Qβ, respectively, c (44.9 min) = broken VNPs, d (53 min) = click reaction reagents (ascorbate, ligand). (G) SEC of Qβ-PEG-C_{60} after purification (red line = 260 nm, pink line = 280 nm). vs. Qβ (dark blue line = 260 nm, light blue line = 280 nm). (H, I) Coomasie gel showing coat proteins and western blot using anti-C_{60} specific antibodies. 1 = CPMV-C_{60}, 2 = CPMV, 3 = Qβ-C_{60}, 4 = Qβ. (J) Hydrodynamic radius as determined by DLS. (K) Coomassie gel showing the coat proteins: 5 = Qβ, 6 = Qβ-azide, 7 = Qβ-PEG-C_{60} (aggregate, peak a of Panel F), 8 = Qβ-PEG-C_{60} (intact

VNPs, panel G), (L) Hydrodynamic radius determined by DLS. * Differences were significant with $p < 0.05$. (M, N) TEM of uranyl acetate-stained VNP-C_{60} conjugates. (O) STEM of osmium-tetroxide-stained Qβ-C_{60} conjugates. Arrows indicate heavily stained C_{60} nanoparticles bound around the equators of Qβ particles. (P) TEM of uranyl acetate-stained Qβ-PEG-C_{60} conjugates. (Q) STEM of OsO_4-stained Qβ-PEG-C_{60} conjugates. Inset reveals higher loading of VNPs with C_{60} nanoparticles, indicated by dots of bright contrast.

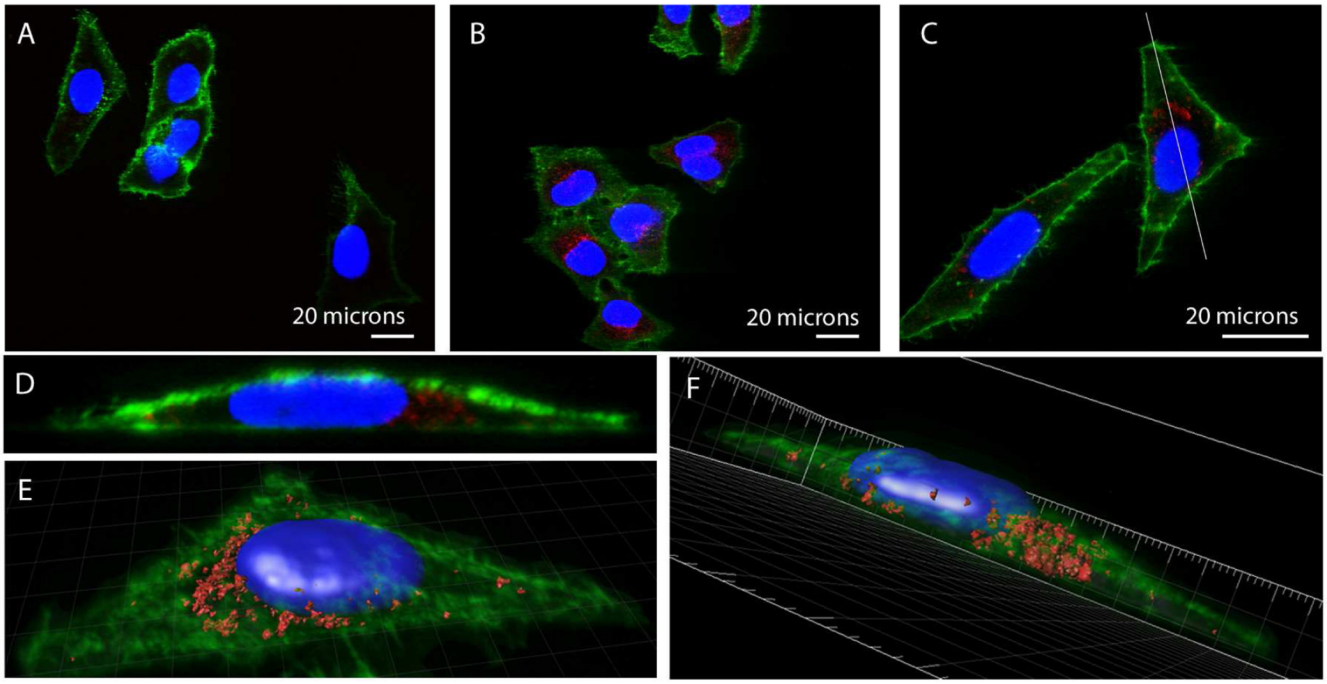

Figure 2.

Confocal microscopy. (A) HeLa cells only. (B–F) Cells treated with Qβ-PEG-C_{60}-A568 particles. Blue = nuclei (DAPI), red = Qβ-PEG-C_{60}-A568, green = WGA-A488. (D) Z-section image (1.2 μm deep) recorded along the line shown in C; step size 0.3 μm. (E,F) Same cell as shown in D, image reconstructions using Imaris software.